Dear editor,

We like to express our appreciation to the reviewers for their comments. We are resubmitting the revised version of the paper number PIP–21–281. We have studied the comments of the reviewer carefully, and have changed the text according to the comments they have listed. Below we refer to each of the reviewer's comments.

## Response to Reviewer #1

**Comment 1.** *A solar cell with BSF is chosen as the basis of the work, claiming that "BSF is one of the popular designs used for industrial mass production...", but this is no longer the case, BSF solar cells are present in the market due to old manufacturing lines that are still operative, but the standard now is PERC technology. If the training of the network is based on SCAPS simulations, why was not trained with a PERC structure? At least, some hint on how results would be with a PERC structure should be given. (By the way, the BSF in this work is made with B-doping, which is also a minoritary approach at the industrial level, where BSF is of Aluminium).*

**Reply:** The Reviewer is absolutely right that PERC technology will be dominant in near future. But now the part of BSF solar cells is still big enough — see Fig. 1.

SCAPS-1D is a one-dimensional solar cell simulation program, so to model PERC solar cells with a rear contact, which is inhomogeneous in a surface, is a rather hard job. We understand the restrictions of 1D simulators and point out this fact in the Conclusion.

We agree that it would be better to use an Al-doped $p^+$-layer, but our choice was determined by the following considerations. The simulated IV curves were used to obtain the ideality factor $n$. According to the two-diode model we applied, $n$ characterizes the current of the second (or so-called recombination) diode which arises due to recombination occurring mainly within the depletion region [2, 3]. The probable $p^+$–layer influences this process mostly via the electric field. Therefore, the kind of doping atom in the $p^+$–layer is not very important for our simulation. In the case of $n^+ - p - p^+$ structure with Al-doped base, a new dataset will be certainly required for training DNN. However, the deep-learning oriented approach for determining impurity concentration that we propose remains quite applicable. Besides, the recombination in the rear surface region is not crucially important for estimating the ideality factor. In our opinion, the trained DNNs can be applied to PERC solar cell in which i) the base is boron-doped; ii) the

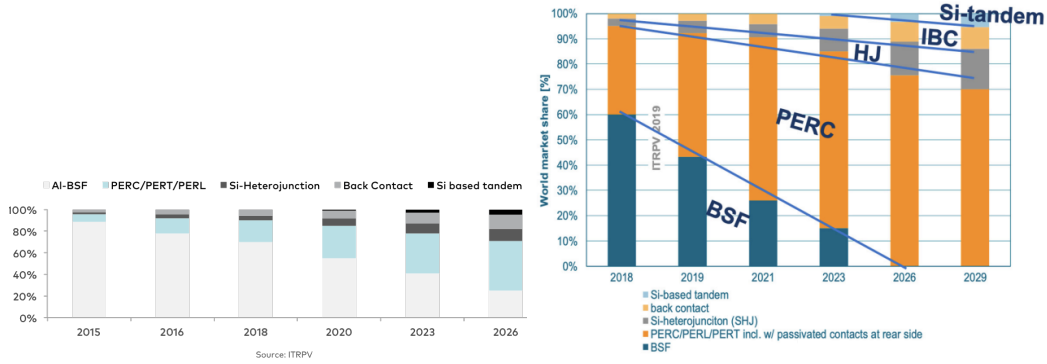


**FIGURE 1** Projected manufacturing capacity share of different silicon–based cell technologies. Sources: https://www.aleo-solar.com/perc-cell-technology-explained/ (left panel), [1] (right panel).

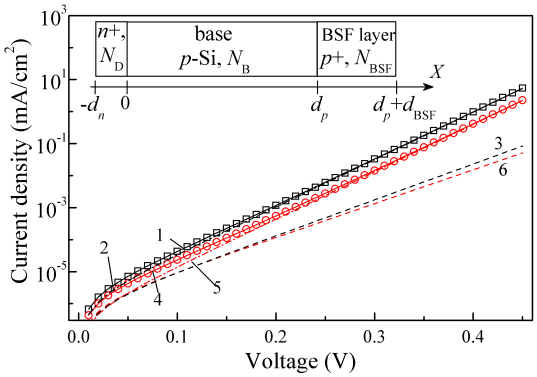


**FIGURE 2** Simulated IV characteristic (marks) and its fitting by Eq. (1) (solid lines 1 and 4). The dashed (3, 6) and dotted–dashed (2, 5) lines represent the recombination diode currents and the "ideal" diode currents, respectively. $N_B = 10^{17}$ cm$^{-3}$, $N_{Fe} = 10^{13}$ cm$^{-3}$, $T = 340$ K, $d_p = 180$ $\mu$m. The results for Fe-case (circles, curves 4-6, red) and Fe-FeB case (squares, curves 1-3, black) are presented. Inset: Structures, which are used in the simulation.

iron-related deep levels are the main cause of defect-assisted recombination.

The text was revised and some speculations about applicability of the trained DNNs were added (last three paragraph before Conclusion).

**Comment 2.** *As far as I understand, the simulation with SCAPS could be improved: emitter and BSF are uniform and this is not the case in reality. There is no mention to the metallization, are there no contacts? There should be, and they will influence the carrier transport and also the surface recombination velocities in the metal-semiconductor interface, among others.*

**Reply:** For metal contacts on the rear and front surfaces, the flat bands' conditions were assumed. The appropriate sentence was added to the text. It should be noted that it is a common practice in SCAPS simulation not to pay much attention to contacts in case they do not create additional barriers — e.g., see [4, 5, 6, 7, 8].

We share the Reviewer's view on the way of improving SCAPS simulation. In the present paper, we concentrate on recombination in the SC base region, which mainly determines the ideality factor. As for the non-uniformities of emitter and BSF-layer, their effect on $n$ is much weaker. In any case, the Reviewer's suggestion is very valuable, and we are going to consider it in the future.

**Comment 3.** *Why a voltage sweep restricted to 0.45 V? This is rather low when compared to the voltages at the maximum power point of BSF solar cells... Wouldn't it influence in the extraction of the ideality factor values?*

**Reply:** In order to fit the simulated data the two-diode model was used, according to which the dark SC current is

given by

$$I = I_{01}\left[\exp\left(-\frac{q(V-R_sI)}{kT}\right)-1\right]+I_{02}\left[\exp\left(-\frac{q(V-R_sI)}{nkT}\right)-1\right]+\frac{V-R_sI}{R_{sh}}, \quad (1)$$

where $I_{01}$ and $I_{02}$ are saturation currents, $R_{sh}$ and $R_s$ are shunt and series resistances. The two-diode model is often applied to describe real Si SCs: in Eq. (1) the first diode represents the "ideal" diode and the first term in the equation describes recombination in the base depth and emitter, including their surfaces; the second diode is the so-called recombination diode and the second term describes recombination within the depletion region [2].

Typical IV curves are shown in Fig. 2. It is seen that the contribution of recombination diode current is essential at low bias only. At $V \simeq 0.25$ V the first term in Eq. (1) is by an order of magnitude greater than the second one (see difference between the dotted-dashed fitting line and dashed fitting line). A similar situation is observed for experimental IV curves — see Fig. 9 in Manuscript. The ideality factor correlates with the slope of the recombination current plotted against the voltage in a semi-logarithmic scale. Therefore the voltage range $(0-0.45)$ V is quite sufficient for determining the ideality factor quite accurately.

The information was added on page 5, the first paragraph from the top; the typical IV curves was added in Supplementary Material.

**Comment 4.** *I am not sure that I interpret well the results in table 5. In the text the authors state that "the results even exceed expectations". But what I see is that the predictions fail in general, largely for the trained dataset cases, but also for the full dataset. There is some discussion on why $DNN_{FeFeB-Fe}$ performs worse than $DNN_{FeFeB}$ and that is Ok... but $DNN_{FeFeB}$ also fails in many cases, isn't it? (temperatures higher than 300K for the higher Fe content, 100% or more error for the training dataset...).*

**Reply:** On the one hand, the Reviewer is right. Unfortunately, DNNs trained by synthetic data proved incapable of measuring iron concentration with high precision in real solar cells (with a certain mismatch between real parameters and those used in the simulation). From this point of view the "glass is half empty".

On the other hand, there are also some reasons to say that the "glass is half full". First of all, in our opinion, the low cost express method which uses a widely applied setup and is able to estimate approximately the range of iron concentration (even with 100% error) can be quite useful. At the same time there are possible ways to improve precision and these are discussed in the Conclusion. Moreover, the results in Table 5 prompt how this method can be appropriately used in practice. First, the near room temperature of IV measurement is preferable (this conclusion is similar to those drawn from the analysis of synthetic IVs); second, the time between FeB pair dissociation and IV measurement must be as short as possible. Finally, in some cases (300 K, "full" dataset) the $DNN_{FeFeB}$ can yield acceptable results.

We hope that the retrieval of deep level parameters from the current–voltage curve by deep learning will be further improved.

**Comment 5.** *In the jargon, we do not talk of surface resistance, but sheet resistance. Also, it is the first time that I read the "anti-recombination isotype barrier" for a high-low junction or a BSF.*

**Reply:** The Reviewer is absolutely right. We have revised the text accordingly.

**Comment 6.** *It is mentioned in the paper that there is Suplementary Material, but I have not had the opportunity to read it.*

**Reply:** We apologize for the embarrassment, but there must be some technical confusion: Reviewer #2 mentioned the data in the table of Supplementary Material.

**Comment 7.** *On the other hand, the paper needs a thorough revision of English, preferably by a native or bilingual speaker. English is not my mother tongue, but I think that there are many expressions that are not correct, and make the reading difficult. From the abstract ("The low-cost and express...", "an ideality factor values"...) to the conclusions ("not numerous input parameters can be multiplied and transformed to the picture and apply a vision model..."(?), and a lot in between: "both for microelectronics, logic technologies and solar cells", "the various semiconductor barrier structures", "practical using", "Fours", "SFB", "in our further calculation", "simulated with using", "in comparing with", "more narrow", etc. etc.*

**Reply:** We are sorry for our English. The text has been revised by a bilingual speaker, and we hope for the language improvement.

## Response to Reviewer #2

**Comment 1.** *2 Simulation details*

*It is assumed that all SRH recombination in the device come from iron impurities and the associated deep level defects. It seems necessary to discuss its validity, and it could be interesting to put it against the fact that Al-BSF devices based on Czochralski silicon wafers are considered. More generally, if another type of defects is present in the solar cell, also inducing SRH recombination, is it possible to estimate to what extend are the DNNs trained here still accurate ?*

**Reply:** The speculations about the applicability of the trained DNNs to different SC structures must be based on assumption that the ideality factor distinguishes depletion-region recombination from most other sources of recombination [2, 3]. Certainly, there are some deviations from this rule for real structures. For instance, our simulation reveals the $n$ dependence on base thickness [9]. Nevertheless this dependence is weak, and the ideality factor value is mainly determined by depletion-region recombination.

Also, the DNNs applicability depends on the requirement for Shockley–Read–Hall recombination to be predominant. In case, if there are other mechanisms causing free carrier concentration to decrease, the models which diverge from the two-diode one are proposed (e.g., three-diode [10, 11]). Moreover, the base must be doped by boron. For example, if SC is prepared from Si:Al wafer, the simulation model which is used for training dataset preparation must be modified: the parameters of $Fe_iAl_s$ pair as well as the changes in defect distribution (Eq. (9)) should be taken into consideration. Finally, if another type of defect (in addition to iron–related deep levels) is present in the solar cell, which also induces intensive SRH recombination, the simulation model must be more complicated as well. The primary competitors of $Fe_iB_s$ are boron-oxygen complexes [12, 13] and oxide precipitates [14, 15] in Cz-Si. So the development of the corresponding model can be our next step. To the point, it should be noted that a high $n$ value can serve as an indicator of another defect presence: in our simulation this value is $n < 1.4$. The absence of non-iron

active defects may be the most limiting factor of the DNNs applicability; in particular, this confined the selection of SCs for our experimental verification of the proposed method.

Thus, the trained DNNs can be applied to BSF solar cells prepared from Si:B wafers. It should be noted that the modern technique of crystal growth makes it possible to restrict oxygen concentration substantially even in solar grade Cz-Si. On the one hand, Al is used to produce the doped $p^+$ region at the industrial level [1, 16]. However, boron BSF is one of the promising techniques for achieving high quality back contact [17, 18] and for this reason the $p^+$ layer, which is doped by boron, was under our consideration. On the other hand, the probable $p^+$–layer influence on the depletion-region recombination process is determined mainly by the electric field. Therefore, the kind of doping atom in $p^+$–layer is not very important for simulation, and in our opinion, the DNNs is applicable for Al BSF cell as well.

Our speculations concerning this issue were added to the Manuscript ( the last three paragraphs before Conclusion).

**Comment 2.** *When Fe-FeB and Fe cases are presented, it could be clearer to provide very few more explanations on both types of defects, and the important fact that iron-boron pairs can be temporarily dissociated, providing the Fe case, through the heat treatment or high illumination already mentioned.*

**Reply:** The corresponding corrections were made on page 4, the third paragraph from the top.

**Comment 3.** *3 Deep neural network models*

*It is clear how the main training dataset is created, and how the 4 * 9 * 11 * 19 = 7524 IV curves are generated. However, the definition of the test datasets and the values for temperature, base thickness, iron concentration and doping level are not clear for each T-varied, d-varied, etc. test set.*

**Reply:** As an example, we added the parameter values used for creating Fe-varied dataset in the last paragraph on page 5 and the first paragraph on page 6.

**Comment 4.** *For instance, in the case of the T-varied test set, it is mentioned that the same base thickness, iron concentration and doping level values are used as in training dataset. However, 4 * 9 * 19 = 684 and the amount of 894 IVs can't be explained by multiplying with any number of temperature values. In Supplementary Material, the associated summary table do neither explain this value 894. More generally these tables are difficult to interpret. It is possible that the subset of 144 values for T-varied test has been duplicated.*

**Reply:** The Reviewer is right: i) the subset of 144 values for the T-varied test dataset has been duplicated; ii) Table in Supplementary Material has mistakes and is not clear. The correct values of $d_p$, $N_B$, $T$, and $N_{Fe}$ were listed in Table, but there were problems with addition and multiplication and we apologize for being inattentive. The Table in Supplementary Material has been revised.

**Comment 5.** *4 Results and discussion*

*On figures 4, 5, 6 and 7, very interesting results are presented, and analyses of the dependence of estimation error with temperature, boron or iron densities and base thickness are well done. However, it seems that the same error statistics of results obtained on test datasets (instead of training dataset) would more directly assess the quality of predictions by the DNNs. For instance, the Fe-varied dataset has been identified to be the closest to "real demand" or results obtained with the all-varied dataset would also be most probably very useful. Such results could be showed in Supplementary Material, in the same form as figures 4, 5, 6 and 7.*

**Reply:** The Supplementary Material has been completed by the figures that represent similar results for test datasets (Figs. 8S–11S).

However, it should be noted that error statistics for the training dataset is more correct and informative. For instance, let us consider the temperature dependence (Fig. 4(a)). In fact, averaging over 684 values was performed for each of 11 points in the training dataset, and in fact these values correspond to the data uniformly distributed over used $(N_{Fe}, N_B, d_p)$-space.

In contrast, only 55 IV characteristics correspond to $T = 295$ K in the Fe-varied dataset (see Table in Supplementary Material). In the All-varied dataset, the six temperature values that have been used are in the range $290 - 315$ K and only three values are in the range $315 - 340$ K. Moreover, eight IV characteristics were simulated at $T = 293$ K for $N_{Fe} = (5 - 9) \times 10^{12}$ cm$^{-3}$ (high values) whereas 60 ideality factor values are available at $T = 292$ K, with $N_{Fe} = 1.1 \times 10^{10} - 5 \times 10^{12}$ cm$^{-3}$ being used to simulate corresponding IV curves. So, it does not seem quite correct to compare data at $T = 292$ K with data at $T = 293$ K.

## References


[1] Green MA. Photovoltaic technology and visions for the future. Prog Energy 2019 Jul;1(1):013001.

[2] Breitenstein O. Understanding the current-voltage characteristics of industrial crystalline silicon solar cells by considering inhomogeneous current distributions. Opto–Electronics Review 2013 Sep;21(3):259–282.

[3] McIntosh K, Altermatt P, Heiser G. Depletion–region recombination in silicon solar cells. When does $mDR = 2$? In: 16th European Photovoltaic Solar Energy Conference: Proceedings of the International Conference and Exhibition Publisher:James and James (Science Publishers) Ltd; 2000. p. 250–253.

[4] Hu ET, Yue GQ, Zhang RJ, Zheng YX, Chen LY, Wang SY. Numerical simulations of multilevel impurity photovoltaic effect in the sulfur doped crystalline silicon. Renewable Energy 2015 May;77:442–446.

[5] Hamache A, Sengouga N, Meftah A, Henini M. Modeling the effect of 1 MeV electron irradiation on the performance of $n^+$-p-$p^+$ silicon space solar cells. Radiat Phys Chem 2016 Jun;123:103–108.

[6] Cappelletti MA, Casas GA, Cédola AP, y Blancá ELP, Soucase BM. Study of the reverse saturation current and series resistance of p-p-n perovskite solar cells using the single and double-diode models. Superlattices Microstruct 2018 Nov;123:338–348.

[7] Azri F, Meftah A, Sengouga N, Meftah A. Electron and hole transport layers optimization by numerical simulation of a perovskite solar cell. Solar Energy 2019 Mar;181:372–378.

[8] Chowdhury MS, Shahahmadi SA, Chelvanathan P, Tiong SK, Amin N, Techato K, et al. Effect of deep-level defect density of the absorber layer and n/i interface in perovskite solar cells by SCAPS-1D. Results Phys 2020 Mar;16:102839.

[9] Olikh OY, Zavhorodnii OV. Modeling of ideality factor value in $n^+$–$p$–$p^+$–Si structure. Journal of Physical Studies 2020;24(4):4701.

[10] Hallam BJ, Hamer PG, Bonilla RS, Wenham SR, Wilshaw PR. Method of Extracting Solar Cell Parameters From Derivatives of Dark I–V Curves. IEEE Journal of Photovoltaics 2017 Sep;7(5):1304–1312.

[11] Shah JM, Li YL, Gessmann T, Schubert EF. Experimental analysis and theoretical model for anomalously high ideality factors ($n \gg 2.0$) in AlGaN/GaN p–n junction diodes. J Appl Phys 2003 Aug;94(4):2627–2630.

[12] Lindroos J, Savin H. Review of light-induced degradation in crystalline silicon solar cells. Sol Energy Mater Sol Cells 2016 Apr;147:115–126.

[13] Niewelt T, Schöon J, Warta W, Glunz SW, Schubert MC. Degradation of Crystalline Silicon Due to Boron–Oxygen Defects. IEEE Journal of Photovoltaics 2017 Jan;7(1):383 –398.

[14] Murphy JD, McGuire JD, Bothe K, Voronkov VV, Falster RJ. Minority carrier lifetime in silicon photovoltaics: The effect of oxygen precipitation. Sol Energy Mater Sol Cells 2014 Jan;120:402–411.

[15] Chen L, Yu X, Chen P, Wang P, Gu X, Lu J, et al. Effect of oxygen precipitation on the performance of Czochralski silicon solar cells. Sol Energy Mater Sol Cells 2011 Nov;95(11):3148–3151.

[16] Wilson GM, Al-Jassim M, Metzger WK, Glunz SW, Verlinden P, Xiong G, et al. The 2020 photovoltaic technologies roadmap. J Phys D: Appl Phys 2020 Sep;53(49):493001.

[17] Kim DS, Nakayashiki K, Rounsaville B, Meemongkolkat V, Rohatgi A. Silicon solar cells with boron back surface field formed by using boric acid. In: 22th European Photovoltaic Solar Energy Conference: Proceedings of the International Conference and Exhibition; 2007. p. 1730–1733.

[18] Du G, Chen B, Chen N, Hu R. Efficient Boron Doping in the Back Surface Field of Crystalline Silicon Solar Cells via Alloyed-Aluminum–Boron Paste. IEEE Electron Device Letters 2012;33(4):573–575.